AIAA JOURNAL
Vol. 40, No. 10, October 2002

Impact Response of Adaptive Piezoelectric Laminated Plates

Dimitris A. Saravanos*
University of Patras, 265 00 Patras, Greece
and
Andreas P. Christoforou†
Kuwait University, 13060, Kuwait

Semi-analytical models for the impact response of composite plates having distributed active and sensory piezoelectric layers are presented. An exact Ritz model is utilized based on a mixed-field piezoelectric laminate theory that encompasses both displacement and electric displacement fields through the laminate. The governing equations of motion of a simply supported plate and a low-velocity impactor are formulated including impactor dynamics and contact law. State feedback linear quadratic regulator and output feedback controllers are implemented to actively reduce impact force. Numerical results quantify the electromechanical response of a composite plate with piezoelectric sensors impacted by three different mass impactors. The impact response of an actively controlled plate is also shown, and the possibility to improve critical impact parameters is demonstrated.

Introduction

IMPACT is a common threat in many structural applications generating large forces that can cause damage in mechanical components. In composite structures even low-velocity impact events can induce hidden damage consisting of delaminations, matrix cracking, and fiber breakage. Such types of damage increase the safety risk and reduce the effectiveness of composite structures as load-bearing members. It is very desirable, therefore, to find new approaches that can reduce the severity of impact damage and/or help in identifying the impact event. Adaptive piezoelectric composite laminates with embedded piezoelectric actuators and sensors might be good candidates for mitigating impact effects as well as for impact parameter identification and damage monitoring and assessment.

Although substantial efforts have been directed towards the analysis and dynamic response of piezoelectric composite laminates and structures,[1,2] it seems that the impact of piezoelectric composite plates has received little attention, mainy in impact load and location identification.[3] Similarly, significant efforts have been reported on active vibration control with adaptive piezoelectric structures,[4–9] and yet it seems that the active control of impact has received minimal attention, and most of the work is mainly in the area of controlling impact in robotic manipulators.[10–12] In robotics, however, the impacting body is controlled, whereas in the case of structural impact by a foreign object the control action should be on the target and not the impactor. This situation presents a different problem and can pose certain challenges in controlling the impact event because key states, such as the impact location and impactor dynamics, might be unknown. Birman et al.[13] proposed the use of shape memory alloys to reduce the deflections and impact damage in composite plates. The results showed a significant reduction in the deflections with moderate reduction in the stresses.

Librescu and Na[14] have reported work on the active control of thin-wall piezoelectric beams subject to blast pulses. Both previous studies assume prescribed impact loading. Yigit and Christoforou[15] have studied the impact control of composite plates using concentrated force actuators with an optimal state feedback strategy. They showed that the control of impact might be possible, provided that all of the states are timely observed and high-speed actuators are available.

Consequently, the present paper investigates the possibility to control impact using distributed piezoelectric actuators and sensors. In this context a semi-analytical model is developed for predicting the electromechanical impact response of piezoelectric plates having distributed active and sensory layers with and without controller interaction. The analytical model combines elements of the so-called mixed-field piezoelectric laminate mechanics,[16] which directly represents all electromechanical state fields in a piezoelectric laminate by combining different kinematic approximations for each field, that is, single-layer kinematic assumptions for the displacements with a layerwise variation of the electric potential. The mechanics naturally capture the effects of actuators and sensors. The governing equations of motion of a simply supported plate and a low-velocity impactor are subsequently formulated including impactor dynamics and contact law[17] in the form of a Ritz solution procedure for predicting the time response of the piezoelectric plate-impactor system using explicit numerical integration. Emphasis is placed on the direct inclusion of impactor-target dynamic interactions and a realistic nonlinear contact law into the model, whereas other nonlinear phenomena, such as damage of the piezoelectric laminate, are left as topics of future study. State and output feedback controllers are incorporated into the model to assess the feasibility of actively controlling low-velocity impact response.

Piezoelectric Plate in Impact

The impacted laminated piezoelectric-composite plate is modeled using the mixed-field piezoelectric laminate theory.[16] In summary, the theory combines first-order shear kinematic assumptions for displacements with layerwise approximation of electric potential through the thickness of the ply. A Cartesian coordinate system $Oxyz$ is defined such that the x and y axes lie on the midsurface, while the z axis is perpendicular to the plane of the laminate. Each ply is a linear piezoelectric material with constitutive equations of the following form:

$$\sigma_i = C_{ij}^E S_j - e_{ik} E_k, \qquad D_l = e_{lj} S_j + \varepsilon_{lk}^S E_k \tag{1}$$

where $i, j = 1, \ldots, 6$ and $k, l = 1, \ldots, 3$; σ_i and S_j are the mechanical stresses and engineering strains in vectorial notation; E_k is the electric field vector; D_l is the electric displacement vector; C_{ij} the elastic stiffness tensor; e_{lj} the piezoelectric tensor; and ε_{lk} is the electric permittivity tensor of the material. Superscripts E and S indicate constant electric field and strain conditions, respectively. The axes 1, 2, and 3 of the material are parallel to the Cartesian coordinate axes x, y, and z, respectively.

Received 24 October 2000; revision received 5 November 2001; accepted for publication 21 April 2002.

*Associate Professor, Department of Mechanical Engineering and Aeronautics; saravanos@mech.upatras.gr. Senior Member AIAA.

†Associate Professor, Department of Mechanical and Industrial Engineering.

Laminate Theory

The implemented mixed-field piezoelectric laminate theory[16] (MPLT) utilizes both displacements and electric potential as generalized state variables and combines different types of through-the-thickness approximations of the state variables (Fig. la). Only some elements of the MPLT theory that are crucial to the formulation are described herein; additional details are provided in Refs. 16 and 18. The displacements and electric potential of the mixed-field theory take the following form:

$$u(x, y, z, t) = u^0(x, y, t) + z\beta_x(x, y, t)$$
$$v(x, y, z, t) = v^0(x, y, t) + z\beta_y(x, y, t)$$
$$w(x, y, z, t) = w^0(x, y, t)$$
$$\varphi(x, y, z, t) = \sum_{j=1}^{N} \varphi^j(x, y, t)\Psi^j(z) \tag{2}$$

where u^0, v^0, w^0 are displacements on the reference surface A_0; superscript j indicates the points z^j at the beginning and end of each discrete layer; ϕ^j is the electric potential at each point z^j; $\Psi^j(z)$ are interpolation functions; and β_x, β_y are flexural rotation angles. The laminate equations of motion are derived by integrating stress and electric displacement equilibrium equations through the thickness of the laminate in terms of generalized forces,

$$N_{1,x} + N_{6,y} - \left(\rho^A \ddot{u}^0 + \rho^B \ddot{\beta}_x^0\right) = 0$$
$$N_{6,x} + N_{2,y} - \left(\rho^A \ddot{v}^0 + \rho^B \ddot{\beta}_y^0\right) = 0$$
$$N_{5,x} + N_{4,y} - \rho^A \ddot{w}^0 = -q_3 \tag{3}$$

generalized moments,

$$M_{1,x} + M_{6,y} - N_5 - \left(\rho^B \ddot{u}^0 + \rho^D \ddot{\beta}_x^0\right) = 0$$
$$M_{6,x} + M_{2,y} - N_4 - \left(\rho^B \ddot{v}^0 + \rho^D \ddot{\beta}_y^0\right) = 0 \tag{4}$$

and conservation of generalized electric charges,

$$D_{1,x}^m + D_{2,y}^m - D_3^m = -\bar{D}_3^m, \qquad m = 1, \ldots, N \tag{5}$$

where q indicates surface traction; subscripts 1, 2, 3 indicate normal components and subscripts 4, 5, 6 indicate shear components; D_3^m overbar is the surface charge flux in the thickness direction at an electrode surface; and ρ^A, ρ^B, ρ^D are the generalized densities, expressing the mass, mass coupling, and rotational inertia per unit area of the laminate, respectively. The preceding equations can form the basis for developing an exact Ritz solution for simply supported laminated piezoelectric plates with orthotropic laminae and piezoelectric layers polarized along the thickness direction ($C_{16} = C_{26} = e_{36} = 0$). By relating the generalized forces N_i, moments M_i, and electric displacements D_i^m to the generalized strain and electric field,[18] the equations for the balance of forces and moments Eqs. (3) and (4) yield five differential equations of the following form:

$$A_{11}S_{1,x}^0 + A_{12}S_{2,x}^0 + B_{11}k_{1,x} + B_{12}k_{2,x} + A_{66}S_{6,y}^0 + B_{66}k_{6,y} - \sum_{m=1}^{N} \bar{E}_{31}^m E_{3,x}^m - \left(\rho^A \ddot{u}^0 + \rho^B \ddot{\beta}_x^0\right) = 0$$

$$A_{66}S_{6,x}^0 + B_{66}k_{6,x} + A_{21}S_{1,y}^0 + A_{22}S_{2,y}^0 + B_{21}k_{1,y} + B_{22}k_{2,y} - \sum_{m=1}^{N} \bar{E}_{32}^m E_{3,y}^m - \left(\rho^A \ddot{v}^0 + \rho^B \ddot{\beta}_y^0\right) = 0$$

$$A_{55}S_{5,x}^0 - \sum_{m=1}^{N} \bar{E}_{15}^m E_{1,x}^m + A_{44}S_{4,y}^0 - \sum_{m=1}^{N} \bar{E}_{24}^m E_{2,y}^m - \rho^A \ddot{w}^0 = -q_3$$

$$B_{11}S_{1,x}^0 + B_{12}S_{2,x}^0 + D_{11}k_{1,x} + D_{12}k_{2,x} + B_{66}S_{6,y}^0 + D_{66}k_{6,y} - A_{55}S_5^0 + \sum_{m=1}^{N} \bar{E}_{15}^m E_1^m - \sum_{m=1}^{N} \hat{E}_{31}^m E_{3,x}^m - \left(\rho^B \ddot{u}^0 + \rho^D \ddot{\beta}_x^0\right) = 0$$

$$B_{66}S_{6,x}^0 + D_{66}k_{6,x} + B_{21}S_{1,y}^0 + B_{22}S_{2,y}^0 + D_{21}k_{1,y} + D_{22}k_{2,y} - A_{44}S_4^0 + \sum_{m=1}^{N} \bar{E}_{24}^m E_2^m - \sum_{m=1}^{N} \hat{E}_{32}^m E_{3,y}^m - \left(\rho^B \ddot{v}^0 + \rho^D \ddot{\beta}_y^0\right) = 0 \tag{6}$$

whereas the generalized charge conservation equation (5) yields N additional equations:

$$\bar{E}_{15}^n S_{5,x}^0 + \sum_{m=1}^{N} G_{11}^{nm} E_{1,x}^m + \bar{E}_{24}^n S_{4,y}^0 + \sum_{m=1}^{N} G_{22}^m E_{2,y}^m - \left(\bar{E}_{31}^n S_1^0 + \bar{E}_{32}^n S_2^0 + \hat{E}_{31}^n k_1 + \hat{E}_{32}^n k_2 + \sum_{m=1}^{N} G_{33}^{nm} E_3^m\right) = -\bar{D}_3^n$$
$$n = 1, \ldots, N \tag{7}$$

where $[A]$, $[B]$, and $[D]$ are the laminate stiffness matrices; $[E]$ overbar and overhat are the laminate piezoelectric matrices representing laminate extension and flexure, respectively; and $[G]$ are the laminate electric permittivity matrices.[18]

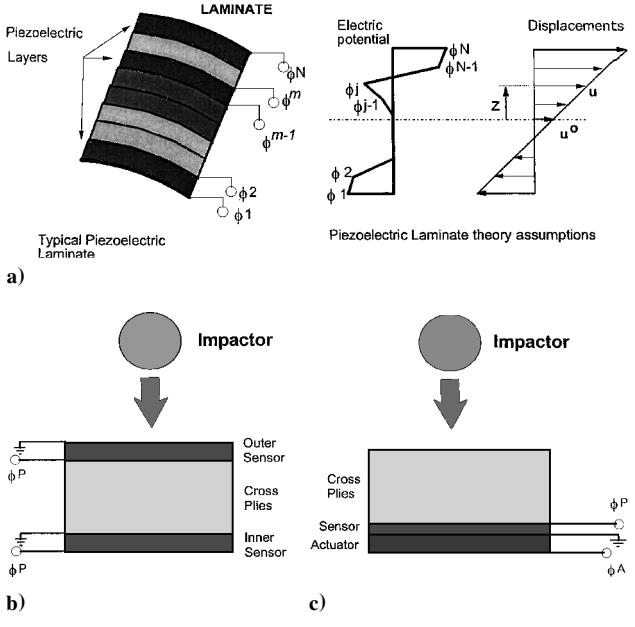

Fig. 1 Piezoelectric laminate: a) typical configuration and mixed kinematic assumptions; b) plate with sensory layers; and c) plate with sensor and actuator.

Plate Equations of Motion

A simply supported rectangular piezoelectric plate is considered, with the origin of the coordinate system $Oxyz$ at the lower-left-hand corner and axes x, y parallel to the sides of the plate. The boundary conditions are $u^0(x, 0) = u^0(x, L_y) = v^0(0, y) = v^0(L_x, y) = w^0(x, 0) = w^0(x, L_y) = w^0(0, y) = w^0(L_x, y) = 0$, and $\Phi^j(x, 0) = \Phi^j(x, L_y) = \Phi^j(0, y) = \Phi^j(L_x, y) = 0$. A fundamental set of solutions satisfying the boundary conditions is

$$u^0(x, y, t) = U_{kl}^0(t)\cos(a_k x)\sin(b_l y)$$
$$v^0(x, y, t) = V_{kl}^0(t)\sin(a_k x)\cos(b_l y)$$
$$w^0(x, y, t) = W_{kl}^0(t)\sin(a_k x)\sin(b_l y)$$
$$\beta_x(x, y, t) = \beta_{xkl}(t)\cos(a_k x)\sin(b_l y)$$
$$\beta_y(x, y, t) = \beta_{ykl}(t)\sin(a_k x)\cos(b_l y)$$
$$\varphi^j(x, y, t) = \Phi_{kl}^j(t)\sin(a_k x)\sin(b_l y)$$
$$a_k = k\pi/L_x, \quad b_l = l\pi/L_y \tag{8}$$

where L_x, L_y are the dimensions of the plate. Thus, the Fourier functions on the right-hand side of Eq. (8) are the actual in-plane vibration mode shapes of the plate; subscripts $k, l = 1, 2, 3, \ldots$ indicate the mode order along x and y axes, respectively, and imply the summation of the mode in the total transient response of the plate; U^0_{kl}, V^0_{kl}, W^0_{kl}, β_{xkl}, β_{ykl}, Φ^j_{kl} represent the participation factors (or amplitudes) of the respective mode in the total response of the plate. Substituting the preceding in-plane mode shapes to the equations of motion Eqs. (6) and (7), collecting the common terms to the unknown state variables, and after partitioning the electric potential to a passive (or sensory) and an active component $\Phi = \{\Phi^1, \ldots, \Phi^N\} = \{\Phi^P; \Phi^A\}$, a set of two linear subsystems, with 5 and N^P discrete equations respectively, results for each mode kl of the following form[18]:

$$[M_{uu}]_{kl}\{\ddot{U}_{kl}\} + [K_{uu}]_{kl}\{U_{kl}\} + \left[K^{PP}_{u\varphi}\right]_{kl}\left\{\Phi^P_{kl}\right\} = \{f_{kl}(t)\} - \left[K^{PA}_{u\varphi}\right]_{kl}\left\{\Phi^A_{kl}\right\} \tag{9}$$

$$\left[K^{PP}_{\varphi u}\right]_{kl}\{U_{kl}\} + \left[K^{PP}_{\varphi\varphi}\right]_{kl}\left\{\Phi^P_{kl}\right\} = \left\{\bar{D}^P_{3kl}(t)\right\} \tag{10}$$

where $\{U\} = \{U^0, V^0, W^0, \beta_x, \beta_y\}$ are the unknown amplitudes of each vibration mode in Eq. (8). Submatrices K_{uu}, $K_{u\phi}$, $K_{\phi\phi}$, and M_{uu} are coefficient matrices depending on the generalized elastic, piezoelectric, permittivity and mass laminate matrices, respectively, and the mode order kl. Superscripts P and A, respectively, indicate passive (or sensory) and active components in accordance with the selected passive and active configuration of piezoelectric layers. The vector $\{f\}_{kl} = \{0, 0, q_{3kl}, 0, 0\}$ includes the Fourier components of mechanical loads and D^P_{3kl} the externally applied charge flux to piezoelectric sensors. Equation (10) describes the conservation of charge and effectively provides the relationship between sensory signal and displacement, which can take different forms depending on the electric conditions imposed on the piezoelectric surfaces. If a sufficiently high electric impedance is connected between the sensor terminals,[18] then there exists practically no external charge flux $[D^P_3(t) = 0]$; in this case sensory electric potential is directly proportional to displacements, and Eq. (10) takes the form

$$\left\{\Phi^P_{kl}\right\} = -\left[K^{PP}_{\varphi\varphi}\right]^{-1}_{kl}\left[K^{PP}_{\varphi u}\right]_{kl}\{U_{kl}\} \tag{11}$$

In the other extreme, when a very low impedance is connected between the sensor terminals the electric permittivity charge component in Eq. (10) becomes negligible. In such case, when electric permittivity is neglected, the time differentiation of Eq. (10) yields that the measured current density J^P between the sensor terminals is proportional to the rate of the displacements:

$$J^P_{kl} = \frac{\mathrm{d}}{\mathrm{d}t}\left\{\bar{D}^P_{3kl}(t)\right\} = \left[K^{PP}_{\varphi u}\right]_{kl}\{\dot{U}_{kl}\} \tag{12}$$

Impactor Dynamics

The case of low velocity impact is considered in this work, where rate effects and perforation are usually neglected. Furthermore, for simplicity and without loss of generality a linear elastic contact law is used, and damage or other nonlinear effects are neglected. The inclusion of damage and penetration in the piezoelectric laminate requires rigorous and extensive developments in many areas, which exceed the scope of this study and are left as topics of future work. When a foreign object of mass m_i transversely impacts the piezocomposite plate at point (x_c, y_c) (see Figs. 1b and 1c), the motion of the impactor is described by

$$m_i \ddot{w}_i(t) = -F_i(t) \tag{13}$$

where w_i is the displacement of the impactor and $F_i(t)$ is the concentrated impact force. The transverse load per unit area applied to the plate is

$$q_3(x, y, t) = F_i(t)\delta(x - x_c)\delta(y - y_c) \tag{14}$$

The impact force $F_i(t)$ is obtained from a linear contact law as

$$F_i(t) = k_y \alpha(t) \tag{15}$$

where k_y is the contact stiffness coefficient that can be calculated from plate and impactor parameters[17] and $\alpha(t)$ is the indentation defined as the relative displacement between the impactor and the plate at the point of contact (x_c, y_c):

$$\alpha(t) = \begin{Bmatrix} w_i(t) - w^0(x_c, y_c, t) & \text{if} \quad w_i(t) - w^0(x_c, y_c, t) \geq 0 \\ 0 & \text{if} \quad w_i(t) - w^0(x_c, y_c, t) < 0 \end{Bmatrix} \tag{16}$$

The transverse plate displacement w^0 is the summation of all modal contributions as they are provided by the solution of Eq. (9) for each mode kl:

$$w^0(x, y, t) = \sum_k \sum_l W^0_{kl}(t) \sin(a_k x) \sin(b_l y) \tag{17}$$

The initial conditions of the impact problem are

$$\{U(x, y, 0)\} = 0, \qquad \{\dot{U}(x, y, 0)\} = 0$$
$$w_i(0) = 0, \qquad \dot{w}_i(0) = v_0 \tag{18}$$

where v_0 is the initial impactor velocity.

Numerical Solution Procedure

The efficient calculation of the impact response, with or without controller consideration, might require substantial computational effort. Equations (9), (10), and (13), which describe the motion of the plate-impactor system, are effectively coupled by the contact law in Eq. (15). Thus, the benefits of the Ritz solution, where a small system of Eqs. (9) and (10) is repeatedly solved for each mode and the final response is calculated from the superposition of all modal contributions, might vanish because of Eqs. (15) and (17), which require knowledge of all modal states of the plate. To overcome this difficulty, the motion equations are solved using an explicit integration scheme, such as the central difference method. Explicit integration schemes calculate the unknown displacements at step $t + \Delta t$ using equilibrium equations at step t. Thus, the contact equation (15) is effectively imposed at step t, where all modal states are already calculated. The calculated impact force ${}^tF$ is then used in Eq. (14) to independently calculate each set of modal state variables ${}^{t+\Delta t}\{U\}_{kl}$, ${}^{t+\Delta t}\{\Phi\}^P_{kl}$ of the plate from Eqs. (9) and (10) and the impactor displacement ${}^{t+\Delta t}w_i$ from Eq. (13). In this manner the advantages of the Ritz method just mentioned are maintained.

Active Impact Control

An obvious application of piezoelectric composite plates might be in active impact control. In this concept the performance of the impacted plate can be improved by feeding back to active piezoelectric layers either state variables or the signals of piezoelectric sensors. Although substantial work has been reported on adaptive piezoelectric structures for vibration control, the development of adaptive piezoelectric plate and controller systems for active impact control involves substantial differences and difficulties for the following reasons: 1) the impactor introduces additional state variables into the plant system; 2) the plate-impactor plant system is nonlinear because of the contact law described by Eqs. (15) and (16); and 3) the primary control objective will be the reduction of impact force, rather than vibration control, as impact force is considered to be directly related to induced damage and reduction of residual strength in the plate. However, the direct reduction of the impact force might not be easily accomplished in practice because the impactor state cannot be monitored directly.

Apparently, the development of such controllers might be a topic requiring substantial work, thus the present work attempts mainly to investigate the feasibility of the concept. It is interesting, therefore, to examine if the impact force can be controlled with piezoelectric actuators using two types of feedback: 1) state feedback and 2) output feedback from piezoelectric sensors. The possibility to design a successful controller using a simplified linear plate-impactor system is also evaluated.

The governing equations of the impactor-plate system can be cast in standard state-space system form:

$$\dot{\boldsymbol{x}} = f(\boldsymbol{x}, t) + [B]\boldsymbol{u}, \qquad \boldsymbol{y} = [C]\boldsymbol{x} \tag{19}$$

where the first equation contains the nonlinear equations of motion, as mandated by Eqs. (9) and (13–16), and the second equation describes the relation of sensory signal (output) to the state, using either Eq. (11) or Eq. (12). The state vector $\boldsymbol{x}$ includes the modal plate velocities and displacement amplitudes and the velocity and position of the impactor, $\boldsymbol{x} = \{\dot{\boldsymbol{U}}_{11}, \boldsymbol{U}_{11}, \ldots, \dot{\boldsymbol{U}}_{mn}, \boldsymbol{U}_{mn}, \dot{w}_i, w_i\}$; the input vector $\boldsymbol{u}$ includes the applied modal voltage amplitudes to the active layers, $\boldsymbol{u} = \{\varphi^A_{11}, \ldots, \varphi^A_{mn}\}$; and the output vector $\boldsymbol{y}$ contains either the modal potential or modal current density of the sensory layers, as mandated by Eqs. (11) or (12), respectively. Although the preceding equations describe the actual plant system, a simplified linear system is also considered for controller design purposes, with identical equations of motion, except that the contact condition in Eq. (16) is relaxed, that is, a contact force $F_i(t) = k_y[w_i(t) - w^0(x_c, y_c, t)]$ is always applied between impactor and plate, irrespectively of the sign of indentation. In this manner the following simplified linear plant system results, which encompasses all impact equations and impactor-target interactions, except those manifested by the nonlinear contact law Eq. (16):

$$\dot{\boldsymbol{x}} = [A]\boldsymbol{x} + [B]\boldsymbol{u}, \qquad \boldsymbol{y} = [C]\boldsymbol{x} \tag{20}$$

The preceding linear system is used for the controller design, which includes impactor-plate interactions. Once the controller is specified, the controller is applied on the actual nonlinear plant system Eq. (19) to evaluate its performance.

State Feedback Control

In this case the input to the piezoelectric actuators is proportional to the state variables

$$\boldsymbol{u} = -[G_x]\boldsymbol{x} \tag{21}$$

where $[G_x]$ is a gain matrix, describing the controller. A linear quadratic regulator (LQR) can be designed with optimal gains, such that the performance index J with quadratic terms on the state and control effort is minimized:

$$J = \frac{1}{2}\int_0^\infty (\boldsymbol{x}^T[Q]\boldsymbol{x} + \boldsymbol{u}^T[R]\boldsymbol{u})\,\mathrm{d}t \tag{22}$$

where $[Q]$ and $[R]$ are weighting matrices. Although a LQR controller might be impractical to implement because it requires knowledge of all states, including impactor position and velocity, an optimal LQR provides the best closed-loop performance. An optimal gain matrix is calculated for the simplified linear plant system Eq. (20), solving a matrix Riccati equation.[19] This gain matrix is subsequently used as the controller of the actual nonlinear plant system Eq. (19).

Output Feedback Control

In this case the input to piezoelectric actuators is proportional to the system output, which includes only signals from piezoelectric sensors:

$$\boldsymbol{u} = -[G_y]\boldsymbol{y} \tag{23}$$

where $[G_y]$ is a suitable gain matrix. Although an output feedback controller is simpler to implement, its development is usually more cumbersome. Formal development of an optimized output feedback controller is possible using either a state estimator or direct prediction of an optimum gain matrix, all in connection with the minimization of performance index J. The present work mainly aims to investigate the feasibility of sensory feedback by trying simple gain matrices, although the formal design of optimized output controllers might be a topic of future work.

Numerical Results

Results and case studies that assess the quality of the developed formulation and quantify the feasibility of active impact control are presented. The numerical studies include 1) impact of a $[(0/90)_2/0]_s$ Gr/epoxy square plate, 2) the response of a $[p^P/(0/90)_2/0]_s$ Gr/epoxy piezoceramic square plate impacted by impactors of various mass, and 3) the active impact control of a $[(0/90)_2/0_2/(90/0)_2/p^P/p^A]$ Gr/epoxy square plate using state and output feedback controllers. The letter p is used in the standard laminate notation to indicate a PZT4 layer, either in sensory (superscript P) or in active (superscript A) configuration. Unless otherwise stated, the dimensions of all plates were assumed $L_x = L_y = 200$ mm, the thickness of each composite ply and piezoceramic layer was 0.270 and 0.250 mm, respectively, and the material properties are shown in Table 1. In all cases it was assumed that the impactor hits the plate at its center ($x/L_x = y/L_y = 0.5$).

Composite Plate

Results of the present method using the described explicit integration scheme are shown for a $[(0/90)_2/0]_s$ Gr/epoxy plate impacted at the center by a spherical impactor of 8.537-g mass and 3.0-m/s initial velocity. Results for this case were first reported by Sun and Chen[20] and have been used since as a benchmark[17] because of the multiple impacts involved. Figure 2 shows the predicted impact force using the present method with 11×11 and 29×29 modes, as well as results reported by Christoforou and Yigit[17] using first-order plate shear theory with rotational inertia terms neglected. The results illustrate the convergence of the present formulation and lead credence to its accuracy.

Piezoelectric Composite Plates

The response of a $[p^P/0/90/0/90/0]_s$ Gr/epoxy PZT4 plate with surface bonded sensory piezoelectric layers covering the whole free

Table 1 Mechanical properties ($\varepsilon_0 = 8.85 \times 10^{-12}$ farad/m, electric permittivity of air)

Property	Gr/epoxy	PZT4
	Elastic properties	
E_{11}, GPa	120	81.3
E_{22}, GPa	7.9	81.3
E_{33}, GPa	7.9	64.5
G_{23}, GPa	5.5	25.6
G_{13}, GPa	5.5	25.6
G_{12}, GPa	5.5	30.6
ν_{12}	0.3	0.33
ν_{13}	0.3	0.43
ν_{23}	0.3	0.43
	Piezoelectric coefficients (10^{-12} m/V)	
d_{31}	0	−122
d_{32}	0	−122
d_{24}	0	495
d_{15}	0	495
	Electric permittivity	
$\varepsilon_{11}/\varepsilon_0$	3.5	1475
$\varepsilon_{22}/\varepsilon_0$	3	1475
$\varepsilon_{33}/\varepsilon_0$	3	1300
	Mass density, kg/m^3	
ρ	1578	7600

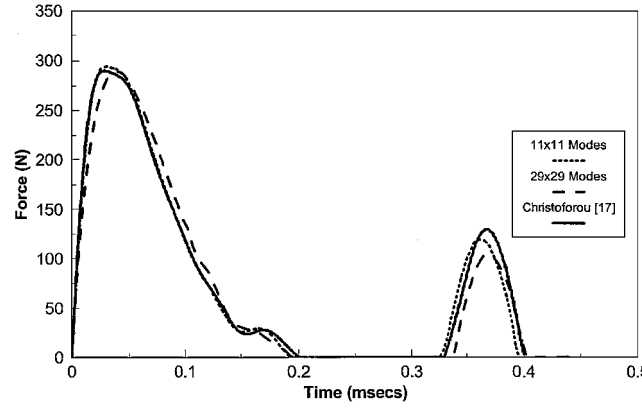

Fig. 2 Impact force of $[(0/90)_2/0]_s$ Gr/epoxy plate impacted at the center by spherical impactor of 8.537-g mass and 3.0-m/s initial velocity.

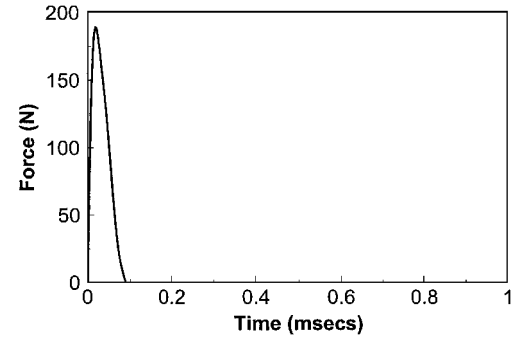

a) Impact force

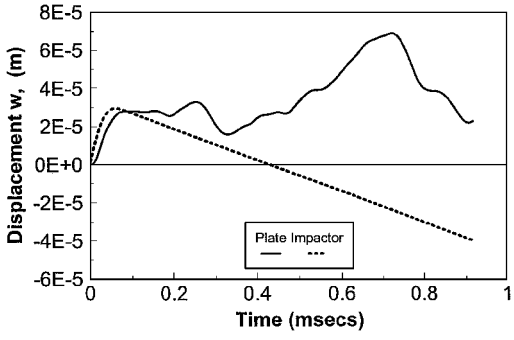

b) Plate and impactor displacement

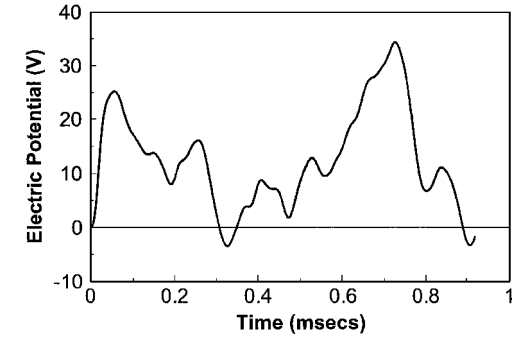

c) Electric potential of piezosensor at center of plate

Fig. 3 Response of $[p/(0/90)_2/0]_s$ Gr/epoxy-PZT4 plate impacted at the center with the 0.008-kg impactor.

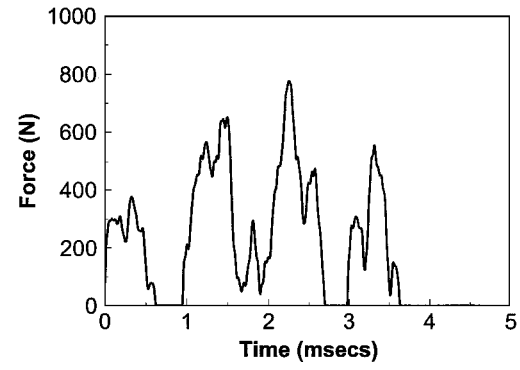

a) Impact force

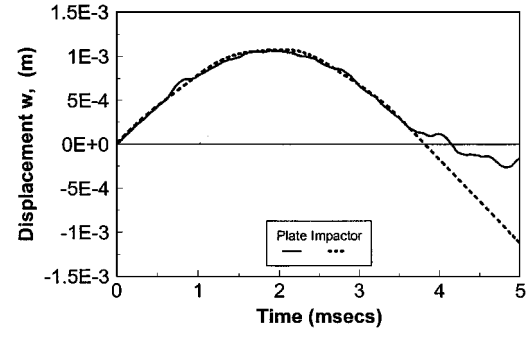

b) Plate and impactor displacement

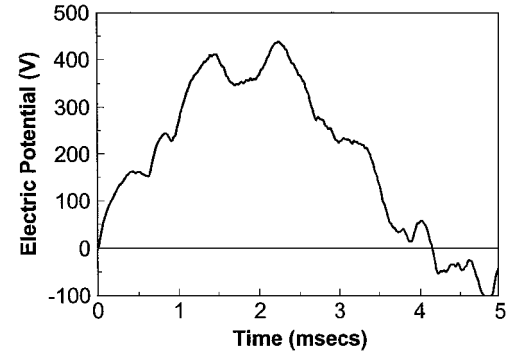

c) Electric potential of piezosensor at center of plate

Fig. 4 Response of $[p/(0/90)_2/0]_s$ Gr/epoxy-PZT4 plate impacted at the center with the 0.5-kg impactor.

area (Fig. 1b) was studied for spherical impactors with 1 m/s initial velocity, having masses of 0.008, 0.500, and 5.00 kg, respectively, and $k_y = 1.234 \times 10^6$ N/m. The considered mass values were selected to correspond to three distinct impact regimes,[17] such that the low mass (8 g) represents an impact controlled mostly by local impactor-plate dynamics, the high mass (5 kg) represents a quasi-static impact case controlled mostly by the global plate stiffness, and the 0.5-kg mass corresponds to the transition regime between the preceding two cases. The first 11×11 combinations of kl modes were used in these analyses.

Figures 3a and 3b show the calculated impact force applied on the plate with the low-mass (0.008-kg) impactor and the associated displacements of the plate and the impactor, respectively. The indentation of the plate by the impactor during the contact period is apparent in Fig. 3b. This is a case of a single impact of very short duration, controlled mostly by the local contact coefficient between the plate and the impactor. After the contact the plate vibrates freely. Figure 3c shows the voltage in the piezoceramic sensor opposite to the impact surface.

Figures 4a and 4b show the predicted response of the plate impacted by the medium-mass (0.5-kg) impactor. This is a transition case where impact is controlled by both local and global stiffness of the plate. There exist multiple contacts between the impactor and the plate, and many modes of the plate seem to participate in the interactions with the impactor. The complexity of the impact is shown in Fig. 4b, where the deflection of the plate is clearly shown to be a superposition of global plate bending and local vibrations resulting in multiple impacts. The voltage signal of the piezosensor is shown in Fig. 4c and clearly accentuates the mixed global-local response characteristics of the impact. The high sensor output is indicative of the sensitivity of piezoceramics and can be scaled down to remain within a desirable range by proper material selection and sensor design, thus avoiding depolarization of the sensor. The value of the developed formulation in identifying and remedying such problems is apparent.

Finally, Figs. 5a and 5b show the impact force and displacements of the plate with the large-mass (5-kg) impactor. Observing Fig. 5b, the displacements of the plate and the impactor seem to practically coincide to a curve approximating the response of a single-degree-of-freedom system with stiffness equal to the global static stiffness of the plate and mass equal to the impactor mass. Such impact cases are known as quasi-static impacts. Yet, the impact force in Fig. 5a shows more complicated dynamics, where local contact stiffness and higher plate modes continue to contribute to the overall response. The response of the PZT4 sensor is shown in Fig. 5c and seems to capture not only the quasi-static response, but also some local contributions of higher modes.

In all three cases the developed method seems to have successfully predicted the impact response of the piezoelectric plate, including all mechanical and electrical states of the plate and the impactor.

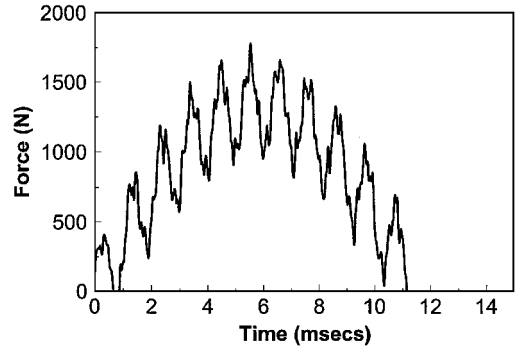

a) Impact force

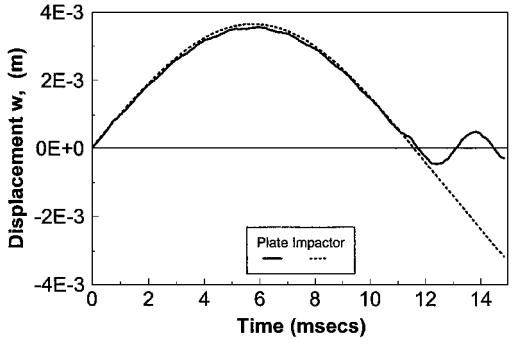

b) Plate and impactor displacement

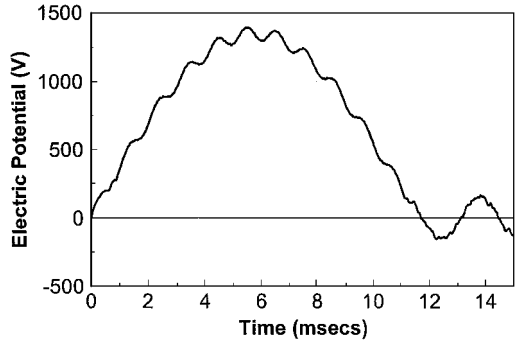

c) Electric potential of piezosensor at center of plate

Fig. 5 Response of $[p/(0/90)_2/0]_s$ Gr/epoxy-PZT4 plate impacted at the center with the 5-kg impactor.

Moreover, the results show that the piezoceramic sensor provides better monitoring of impact dynamics, compared to plate displacement, and might combine information directly related to the impact force. The technical significance of this observation is apparent, considering the associated difficulties in monitoring impact force. An additional issue emanating from these impact studies is the possibility to control impact response, using either state or output feedback to the piezoelectric actuators. The active impact control issue is addressed in the following paragraphs.

Active Impact Control

The impact response of an adaptive $\{[(0/90)_2/0]_s/p^P/p^A\}$ Gr/epoxy plate impacted at the center with a 0.5-kg mass at 1 m/s is considered with $k_y = 1.234 \times 10^6$ N/m. One 0.125-mm sensory and one 0.250-mm active piezoceramic layer were bonded on the opposite to the impact side of the plate with their common interface being grounded (Fig. 1c). The piezoelectric layers were assumed to fully cover the area of the plate. The system response was approximated using 3×3 plate modes. The equations of motion (9) and the structural degrees of freedom were further condensed to the three displacements $\{U\}_{kl} = \{U^0, V^0, W^0\}_{kl}$ by assuming negligible rotational inertias. In the case of central impact, only the odd modes (1, 1), (1, 3), (3, 1), and (3, 3) are excited, thus the plate-impactor system model involves 26 state variables, of which 24 describe the amplitudes of the modal velocities and deflections of the plate. The system inputs are the four amplitudes of the modal electric potential applied to the active layer, $\boldsymbol{u} = \{\varphi^A_{11}, \varphi^A_{13}, \varphi^A_{31}, \varphi^A_{33}\}$. Each active potential input represents the amplitude of one of the spatial modal voltage patterns applied on the surface of the active layer, as described by Eq. (8) and shown in Fig. 6.

LQR Control

Two optimal LQR controllers were designed using the simplified linear system [Eq. (20)] of the preceding model. In each case an optimal feedback gain matrix $[G^*_x]$ was calculated for the linear system (20) and was subsequently used in the actual system Eq. (19). In all cases the weighting matrix $[R]$ was diagonal with all terms equal to 0.001. Two weighting matrices $[Q]$ were used in performance index (22), which respectively force the minimization of the following quadratic expressions: 1) $\boldsymbol{x}^T[Q]\boldsymbol{x} = q_1(w^0 - w_i)^2$, which represents a measure of indentation, and consequently of impact force, and 2) $\boldsymbol{x}^T[Q]\boldsymbol{x} = q_2(\dot{w}^0 - \dot{w}_i)^2$, which represents a measure of the rate of indentation and rate of impact force and also a measure of the momentum difference between the plate and impactor.

The two optimal state feedback gain matrices that were calculated using the indexes defined in the preceding paragraph are identified as LQR1 and LQR2 controllers. Weighting factors $q_1 = 1200$ and

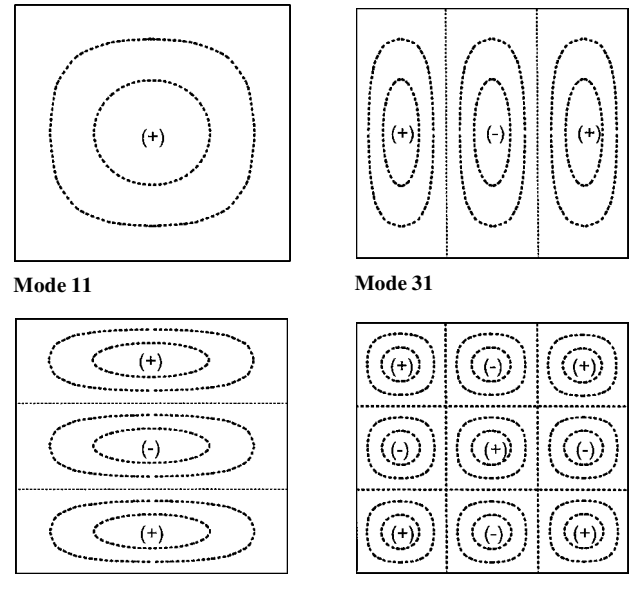

Mode 11 Mode 31

Mode 13 Mode 33

Fig. 6 Modal distributions of applied and sensory electric potential over the area of the plate.

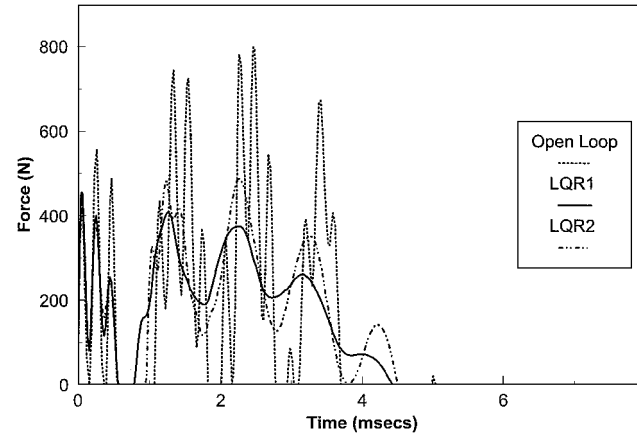

Fig. 7 Impact force of active $\{[(0/90)_2/0]_s/p^P/p^A\}$ Gr/epoxy PZT4 plate: without control; with LQR1 optimized for force minimization; and with LQR2 optimized for relative impactor-plate velocity minimization. Central impact with 0.5-kg mass and 1-m/s initial velocity.

$q_2 = 200$ were selected through a trial and error procedure, such that each active modal potential remained within the range of ± 200 V. The tuning of these weighting factors provides a way to safeguard against high applied voltages, which can depolarize the piezoceramic actuator.

Figure 7 shows the impact force obtained using the gain matrix of the LQR1 controller on the actual plant system [Eq. (19)], which gains were specified to minimize the integral of the impact force of the linear system (20). Figure 7 also shows the impact force obtained using the gain matrix of the LQR2 controller, which was specified to minimize the relative impactor-plate velocity of the linear system Eq. (20). The impact force of the actively controlled plate has been drastically reduced by both controllers, especially during the final impact contacts. LQR1, which was designed to directly reduce indentation, produced the higher force reduction. Figures 8a–8c show the displacements of the plate and the impactor, without control and with the controllers, respectively. The improved contact between the impactor and the actively controlled plates is apparent. Figures 9a and 9b show the inputs to the actuator, which represent the four amplitudes of modal electric potential patterns (see Fig. 6) applied on the active layer. The predicted actuator input response is within the

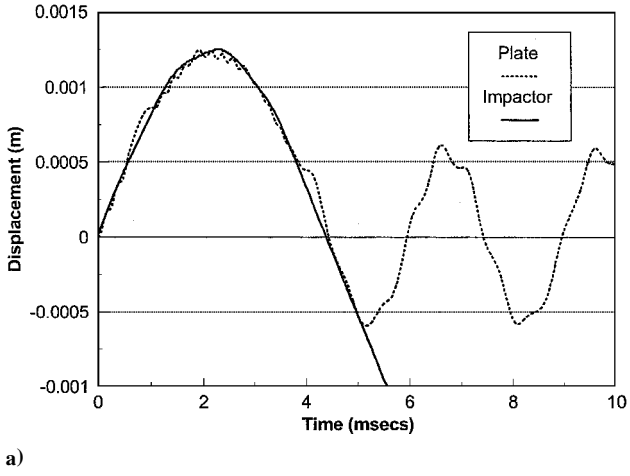

a)

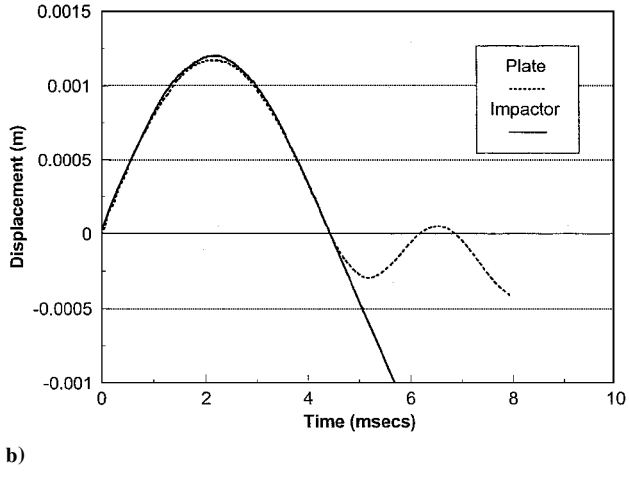

b)

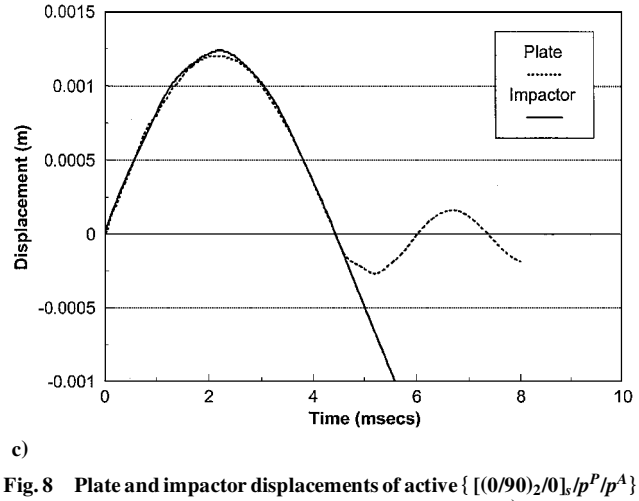

c)

Fig. 8 Plate and impactor displacements of active $\{[(0/90)_2/0]_s/p^P/p^A\}$ Gr/epoxy-PZT4 plate with state feedback controllers a) without controller, b) with LQR1 optimized for force minimization, and c) with LQR2 optimized for relative impactor-plate velocity minimization. Central impact with 0.5-kg mass and 1-m/s initial velocity.

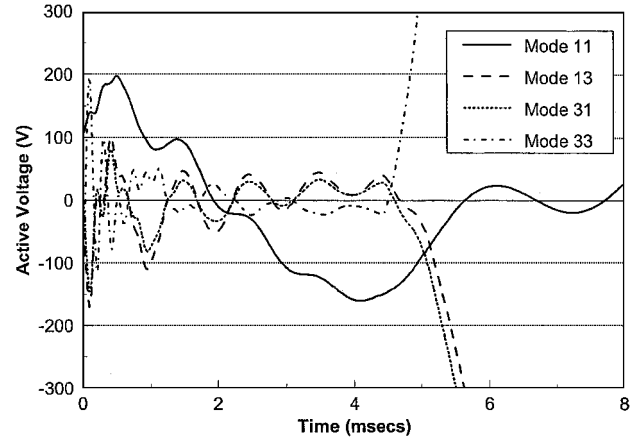

a)

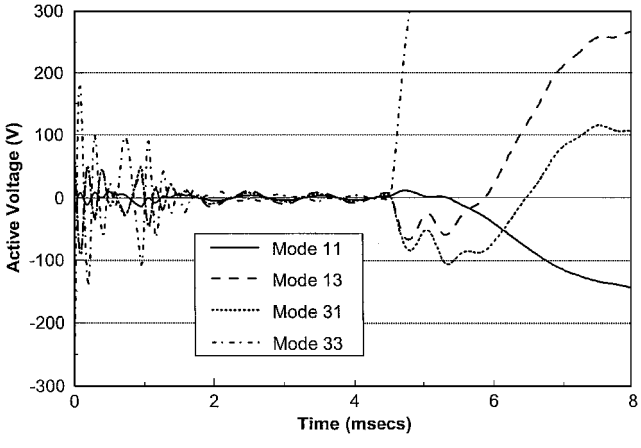

b)

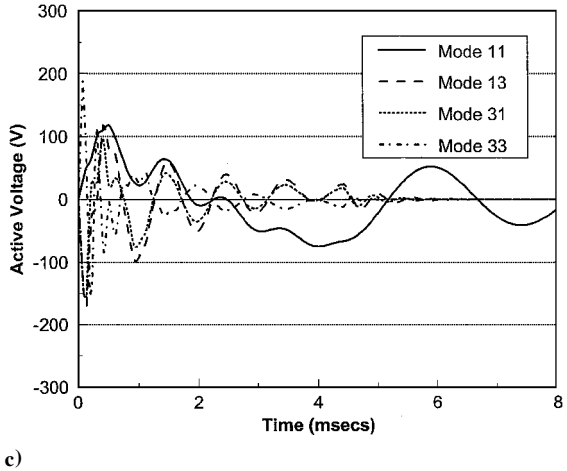

c)

Fig. 9 Applied modal electric potential amplitudes on the actuator of the $\{[(0/90)_2/0]_s/p^P/p^A\}$ Gr/epoxy-PZT4 plate for a) LQR1 controller, b) LQR2 controller, and c) sensory output feedback. Central impact with 0.5-kg mass and 1-m/s initial velocity.

response speed of most piezoceramic materials. All applied electric potential amplitudes remained within the ±200-V range, indicating that the potential problem of excessively high input voltages can be addressed and resolved by the proposed controller design procedure. In both cases the reduction in impact force has been achieved by improving and extending the contact between the impactor and the plate. In the case of LQR1 controller, this seems to have been mostly attained by inducing small active bending deflections in the plate to reduce its relative position to the impactor. This observation is reinforced by the more uniform actuator inputs shown in Fig. 8a and particularly by the higher actuation of the fundamental mode. In the case of the LQR2 controller, the contact was mostly improved by actively damping the plate such that its relative vibration to the impactor was reduced. In both cases energy has been removed from the system through the active layer, as indicated by the highly reduced vibration amplitude of the plate after impact.

The obtained remarkable performance of the LQR controller suffers in practical implementation. It requires measurement and feedback of all state variables, including the impactor position and velocity, and also because of the latter the actuator inputs keep steadily increasing after the termination of impact with undesirable effects. However, the preceding cases illustrated the feasibility of active impact control and validate the proposed approach for LQR controller design using the simplified linear system.

Output Feedback Control

The performance of an output feedback controller was investigated using a diagonal matrix of uniform gains $[K_y] = \text{diag}(k, \ldots, k)$. The system output was considered to be the modal current density amplitudes of the piezoelectric sensor provided by Eq. (12), that is, $\boldsymbol{y} = (J_{11}^P, J_{13}^P, J_{31}^P, J_{33}^P)$ with modal paterns shown in Fig. 6. Figures 10a and 10b, respectively, show the predicted impact force and the plate-impactor displacement for $k = 65$. The results illustrate again the feasibility of drastic reduction in impact force using direct sensory feedback to the piezoelectric actuators. Figure 9c shows the modal electric potential amplitude inputs applied on the active layer.

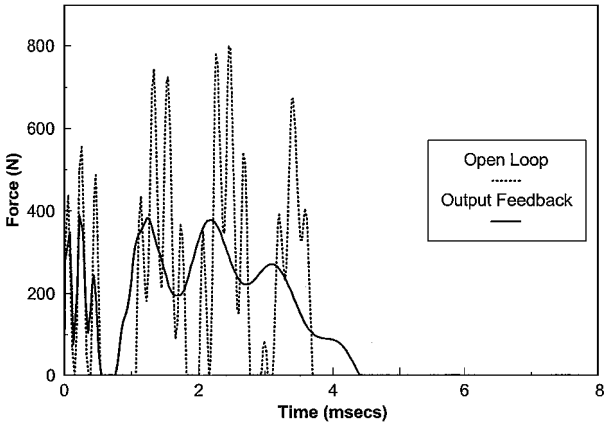

a)

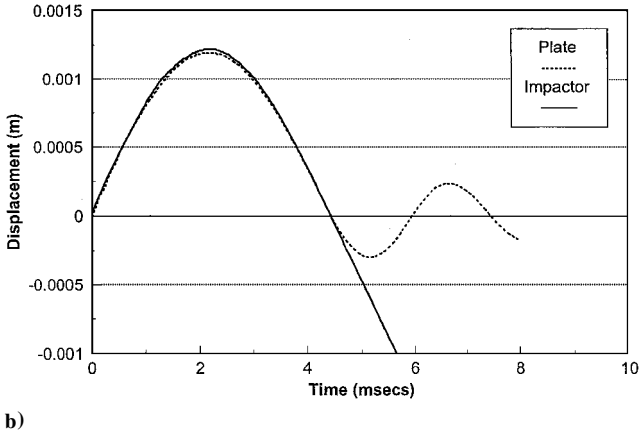

b)

Fig. 10 Impact response of active $\{[(0/90)_2/0]_s/p^P/p^A\}$ Gr/epoxy-PZT4 plate with sensory output feedback: a) impact force and b) plate and impactor displacements. Central impact with 0.5-kg mass and 1-m/s initial velocity.

Overall, the preceding numerical examples suggest that at least in the local-global transition area substantial reductions in impact force can be attained with active piezoelectric structures using either state feedback or sensory output feedback controllers. In all cases the predicted actuator inputs remained within reasonable values that, in terms of frequency bandwidth and amplitude, are within the limits of many common piezoceramics. The results also support the proposed controller development using optimal gain matrices of a simplified linear impact system. The application of the approach to more realistic structural configurations and the development of optimized output feedback controllers are left as topics of future research.

Summary

The low-energy-impact response of composite plates encompassing distributed active and sensory piezoelectric layers was analyzed and predicted. An exact Ritz model was developed, which uses a mixed-field piezoelectric laminate theory representing both displacement and electric potential fields through the laminate. The governing equations of motion of a simply supported plate and a low-velocity impactor were formulated including impactor dynamics and contact effects. An explicit time-integration scheme was developed for the efficient numerical calculation of impact response. State feedback (LQR) and output feedback controllers were implemented to actively reduce impact force. The developed formulation has been encoded into prototype research software.

Numerical evaluations were presented for a composite-piezoelectric plate impacted by three different mass impactors. The impact force, displacement, and sensory voltage responses were quantified. In addition, the impact response of an actively controlled composite-piezoelectric plate using optimized LQR controllers or sensory output feedback was also investigated. In all cases the controller design included interactions of the impactor-plate system, and significant reductions in the impact force were obtained, primarily by actively improving and extending the contact between the impactor and the plate via small plate deflections and/or active damping induced by the piezoelectric actuator. In closing, the results illustrated the feasibility to reduce the impact force using properly designed controllers and active/sensory structures.

Acknowledgment

Most of this work was performed while A. P. Christoforou was on sabbatical leave at the University of Patras. The support of Kuwait University in the form of a sabbatical leave is gratefully acknowledged.

References

[1]Sunar, M., and Rao, S. S., "Recent Advances in Sensing and Control of Flexible Structures via Piezoelectric Materials Technology," *Applied Mechanics Reviews*, Vol. 52, No. 1, 1999, pp. 1–16.

[2]Saravanos, D. A., and Heyliger, P. R., "Mechanics and Computational Models for Laminated Piezoelectric Beams, Plates, and Shells," *Applied Mechanics Reviews*, Vol. 52, No. 10, 1999, pp. 305–320.

[3]Choi, K., and Chang, F. K., "Identification of Impact Force and Location Using Distributed Sensors," *AIAA Journal*, Vol. 34, No. 1, 1996, pp. 136–142.

[4]Bailey, T., and Hubbard, J. E., "Distributed Piezoelectric Polymer Active Vibration Control of a Cantilever Beam," *Journal of Guidance, Control, and Dynamics*, Vol. 8, No. 5, 1985, pp. 605–611.

[5]Baz, A., and Poh, S., "Performance of an Active Control System with Piezoelectric Actuators," *Journal of Sound and Vibration*, Vol. 126, No. 2, 1988, pp. 327–343.

[6]Tzou, H. S., and Tseng, C. I., "Distributed Piezoelectric Sensor/Actuator Design for Dynamic Measurement/Control of Distributed Parameter Systems: A Piezoelectric Finite Element Approach," *Journal of Sound and Vibration*, Vol. 138, No. 1, 1990, pp. 17–34.

[7]Chandrashekhara, K., and Agarwal, A. N., "Active Vibration of Laminated Composite Plates Using Piezoelectric Devices: A Finite Element Approach," *Journal of Intelligent Material Systems and Structures*, Vol. 4, No. 4, 1993, pp. 496–508.

[8]Ray, M. C., "Optimal Control of Laminated Plate with Piezoelectric Sensor and Actuator Layers," *AIAA Journal*, Vol. 36, No. 12, 1998, pp. 2204–2208.

[9]Liu, G. R., Peng, X. Q., Lam, K. Y., and Tani, J., "Vibration Control Simulation of Laminated Composite Plates with Integrated Piezoelectrics," *Journal of Sound and Vibration*, Vol. 220, No. 5, 1999, pp. 827–846.

[10]Volpe, R., and Khosla, P., "A Theoretical and Experimental Investigation of Impact Control for Manipulators," *International Journal of Robotics Research*, Vol. 12, No. 4, 1993, pp. 351–365.

[11]Tornambe, A., "Global Regulation of a Planar Robot Arm Striking a Surface," *IEEE Transactions on Automatic Control*, Vol. 41, No. 10, 1996, pp. 1517–1521.

[12]Weng, S. W., and Young, K., "An Impact Control Scheme Inspired by Human Reflex," *Journal of Robotic Systems*, Vol. 13, No. 12, 1996, pp. 837–855.

[13]Birman, V., Chandrashekhara, K., and Sukhendu, S., "Global Strength of Hybrid Shape Memory Composite Plates Subjected to Low-Velocity Impact," *Journal of Reinforced Plastics and Composites*, Vol. 16, No. 9, 1997, pp. 791–809.

[14]Librescu, L., and Na, S., "Dynamic Response Control of Thin-Walled Beams to Blast Pulses Using Structural Tailoring and Piezoelectric Actuation," *Journal of Applied Mechanics*, Vol. 65, No. 2, 1998, pp. 497–504.

[15]Yigit, A. S., and Christoforou, A. P., "Control of Low-Velocity Impact Response in Composite Plates," *Journal of Vibration and Control*, Vol. 6, No. 6, 2000, pp. 429–447.

[16]Saravanos, D. A., "Coupled Mixed-Field Laminate Theory and Finite Element for Smart Piezoelectric Composite Shell Structures," *AIAA Journal*, Vol. 35, No. 8, 1997, pp. 1327–1333.

[17]Christoforou, A. P., and Yigit, A. S., "Characterization of Impact in Composite Structures," *Composite Structures*, Vol. 43, No. 1, 1998, pp. 15–24.

[18]Saravanos, D. A., "Damped Vibration of Composite Plates with Passive Piezoelectric-Resistor Elements," *Journal of Sound and Vibration*, Vol. 221, No. 5, 1999, pp. 867–885.

[19]Sage, A. P., and White, C. C., *Optimum Systems Control*, Prentice–Hall, Upper Saddle River, NJ, 1977, pp. 87–123.

[20]Sun, C. T., and Chen, J. K., "On the Impact of Initially Stressed Composite Laminates," *Journal of Composite Materials*, Vol. 19, No. 6, 1985, pp. 490–504.

A. M. Baz
Associate Editor